Research Article

Cornel Cobianu*, Niculae Dumbravescu, Bogdan-Catalin Serban, Octavian Buiu, Cosmin Romanitan, Florin Comanescu, Mihai Danila, Roxana Marinescu, Viorel Avramescu, and Octavian Ionescu

Sonochemically synthetized ZnO-Graphene nanohybrids and its characterization

https://doi.org/10.1515/rams-2020-0013
Received Dec 12, 2019; accepted Jan 23, 2020

Abstract: The paper presents the morphological, structural and compositional properties of the sonochemically prepared ZnO-1.4wt% Graphene (Z-G) nanocomposites as a function of pH value of suspension varying from 8.5 to 14 and thermal annealing at 450°C in nitrogen or air ambient. The SEM analysis of the Z-G hybrids dried at 150°C in air has shown a nano-flower like nanostructure for a pH value of 14. The XRD analysis of dried Z-G hybrids revealed a crystallite size increase from 3.5 nm to 18.4 nm with pH increase, and this result was explained in terms of colloids zeta potential evolution with pH value. The Raman and EDS spectroscopy have shown a split of the G band (1575 cm^{-1}) of graphene into two bands (1575 cm^{-1} and 1605 cm^{-1}), an increased height of D (1323 cm^{-1}) band, and an additional amount of carbon due to CO_2 absorption from the air, respectively. The carbon incorporation increased with the decrease of pH, and was associated with a hydrozincite phase, $Zn_5(CO_3)_2(OH)_6$. The formation of dried Z-G nanocomposite was clearly demonstrated only at a pH value equal to 14, where two ZnO Raman active bands at 314.9 cm^{-1} and 428.2 cm^{-1} appeared. This result may indicate the sensitivity of the Raman spectroscopy to the nanoflower-like nanostructure of dried Z-G hybrids prepared at pH=14. *The thermal treatment of Z-G hybrids in N_2 at 450°C* has increased the number of ZnO Raman bands as a function of pH value, it has decreased the amount of additional carbon by conversion of hydrozincite to ZnO and *preserved the graphene profile*. *The thermal treatment in air at 450°C* has increased the crystalline symmetry and stoichiometry of the ZnO as revealed by high and narrow Raman band from 99 cm^{-1} specific to Zn optical phonons, but it *has severely affected the graphene profile in the Z-G hybrid*, due to combustion of graphene in oxygen from the ambient.

Keywords: ZnO-graphene nanocomposite, nano-flower architecture, sonochemistry, colloids, zeta potential, hydrozincite

1 Introduction

Zinc oxide (ZnO) is a multifunctional n-type metal oxide semiconductor with wide bandgap (3.37 eV) and large exciton binding energy (60 meV) which has been extensively researched in chemiresistive gas sensors [1, 2], piezoelectric nanogenerators [3], photoelectric devices like flat panel display, solar cell, light emitting diodes and laser diodes [4–6]. In addition, due its high photosensitivity, ZnO was also considered a good candidate for novel photocatalysts, and a possible replacement for TiO_2 [7–13].

However, there are material limitations in using ZnO in all the above applications. For example, in chemiresistive gas detection, the use of ZnO as semiconducting metal oxide sensitive layer has required the heating of the substrate for sensor operation, which increased the power consumption for the device operation [1]. Similarly, in active devices, the ZnO semiconductor is very difficult to be prepared as a reproducible p-type semiconductor, and therefore there are challenges in doing p-n homojunctions [14], while as a photocatalyst, ZnO has a very high recombination rate of photogenerated electron-hole pairs, which reduces its efficiency [15].

An important step-forward in improving the functional properties of ZnO was made by mixing it with organic [16] or carbonic materials [17], due to the benefits of

***Corresponding Author: Cornel Cobianu:** National Institute for Research and Development in Microtechnologies-IMT Bucharest, Romania, 126A, Erou Iancu Nicolae Str., 077190 Voluntari, Romania; Academy of Romanian Scientists, 3 Ilfov Str., 50044 Bucharest, Sector 3, Romania; Email: cornel.cobianu@imt.ro, cornel.cobianu@gmail.com
Niculae Dumbravescu, Bogdan-Catalin Serban, Octavian Buiu, Cosmin Romanitan, Florin Comanescu, Mihai Danila, Roxana Marinescu, Viorel Avramescu, Octavian Ionescu: National Institute for Research and Development in Microtechnologies-IMT Bucharest, Romania, 126A, Erou Iancu Nicolae Str., 077190 Voluntari, Romania

the synergy of the hybrids developed by different synthesis methods, which, for example, have drastically reduced the operation temperature of the chemiresistive gas sensors from about 300°C to near the room temperature. On the same direction, ZnO-graphene nanocomposites have been used for the increase of the photocatalytic properties by combining ZnO as a good electron donor with graphene as a good electron acceptor, and thus creating a an effective electron transfer which finally reduced the recombination rate of the photogenerated electron-hole pairs [18].

Further improvements of functional properties of ZnO-carbonic material nanocomposites were obtained by the development of the synthesis methods which have generated nanostructured architectures for these hybrids. For example, in the case of chemiresistive gas sensors, as a result of a high specific area of the nanostructured sensing layer and its increased porosity, the operation temperature and the response time were reduced, while the lifetime of gas sensors was increased [19].

In the early stage of the semiconductor metal oxide-carbonic material composites fabrication, for example, the multiwall carbon nanotube (MWCNT) were thoroughly mixed in water with ready-made SnO_2 nanoparticles of 10-15 nm, in the presence of cetyltrimethylammonium bromide, used as a structuring agent [20]. This SnO_2-MWCNT nanocomposite has shown room temperature sensing properties for the detection of ammonia. The next evolutionary step was the synthesis of the semiconductor metal oxide-carbonic material composite by mixing precursors of the metal oxide (like salt (nitrates, acetates) or acids of the metal) together with aqueous solutions of CNT, or precursors of graphene (graphene oxide), so that an intimate chemical bonding at atomic level to occur between the two components during synthesis. For example, synthesis of WO_3-Reduced Graphene Oxide composite prepared by such a bottom-up approach was demonstrated to provide photocatalytic properties much higher than the same composite obtained by simply mixing WO_3 nanoparticles with graphene [21]. Recently, excellent work on photocatalytic properties of carbonic materials (modified CNT, graphene oxide (GO) [22] and metal oxide (ZnO, Fe_3O_4-ZnO)- carbonic materials composites (SWCNT, MWCNT, GO) [23–28] was published, bringing such materials closer to industrial applications.

However, there is still a research gap concerning novel methods for the metal oxide-carbonic material composites fabrication, with controlled nanostructure as a function of processing parameters. In addition, there is a strong need for understanding the stability of the metal oxide-carbonic material hybrids as a function of annealing gas and temperature, which is of paramount importance in gas sensing applications, where the Z-G composite can be exposed to air at different operating temperatures. For such applications, the ambient temperature can reach higher temperatures, above 250°C.

It is the purpose of this paper to present the results of an experimental study of synthesis and material characterization of the ZnO-Graphene (Z-G) nanocomposite by means of a novel approach, where the nanostructured hybrid was directly obtained by one-pot sonochemical synthesis [29] without the use of growth orientation agents, while the precursors were aqueous solutions of zinc nitrate ($Zn(NO_3)_2 \times 6H_2O$) and pristine graphene nanoplatelets [30] with sodium hydroxide (NaOH) as a precipitation and orientation agent. The control of evolution of the hybrid nanostructure during sonochemical processing as a function of pH of the suspension will be presented, here. In addition, the effect of the thermal treatments in nitrogen or air will show major changes of chemical composition of this Z-G hybrid as a function of specific ambient. It will be shown that the ZnO-Graphene hybrid will preserve the graphene profile after annealing at 450°C in nitrogen, but not in air !. This result should be considered during different applications where the nanocomposite is exposed to higher temperatures in air, with a major influence on chemiresistive gas sensing, where in some cases heating of the ZnO-Graphene nanocomposite in air is needed.

2 Experimental

The sonochemical synthesis was performed in a Hielscher Ultrasonics, UP 200 St apparatus operating at a working frequency of 26 KHz, presented schematically in Figure 1. The maximum electric power of 200 W of the ac generator 1 is converted in acoustic power by an ultrasonic transducer 2 providing a maximum power density of 130W/cm^2 for a sonotrode 3 with the surface area of 1.53 cm^2 which was immersed in water at a depth of minimum 5 mm. The longitudinal vibrations of the sonotrode on the z-direction have a maximum amplitude of 9-240 μm, depending on the type of sonotrode used. The acoustic energy transferred from the sonotrode to the solution is creating acoustic waves manifested as compression and rarefaction regions in the liquid, which end-up with a transient regime of continuous bubble formation and collapse, a process called cavitation. It has been shown that the gas inside these bubbles can reach temperatures of 5000 K and pressures of 1000 bar [29] and their implosion will create local hot spots which are able to trigger water dissociation with free radical formation of $H^{\cdot}$ and $OH^{\cdot}$. These radicals are activat-

ing the liquid phase chemical reactions, as well as solid state crystallization of the newly formed materials. From this brief description, it is obvious that there is no direct interaction of the acoustic radiation with the matter due the immense difference between the wavelength of the acoustic waves and the molecular dimensions. Therefore, all the chemical and physical effects of the sonochemistry come from the cavitation process described above. Such a process has many applications in the synthesis of complex binary, ternary and quaternary hybrids, where efficient sonication and reaction of precursors occur [31, 32]. This is of extreme importance in the case of synthesis of carbonic composites, where the dispersion of CNT's, graphene or carbon nanohorns (CNH) in the matrix is the key of the homogenous hybrid formation.

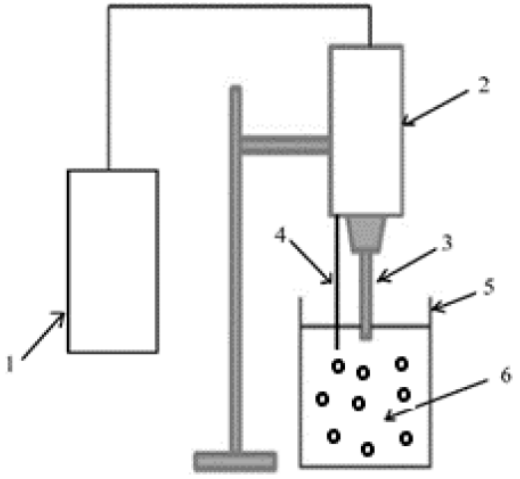

Figure 1: Schematic presentation of the ultrasonic apparatus for sonochemical synthesis. 1=ac generator, 2=ultrasonic converter, 3=sonotrode, 4=Pt100 thermometer, 5=beaker, 6=suspension.

The sonochemically prepared ZnO-Graphene hybrids were obtained by using $Zn(NO_3)_2 \times 6\ H_2O$, purum p.a., crystallized, ≥ 99.0% (KT) from Sigma-Aldrich and a commercial aqueous solution of graphene (0.05 mg/mL) containing flakes with 1-4$^+$ layers of graphene, very well dispersed in the aqueous solution. Such a graphene precursor, delivered by NanoIntegris, has had a homogeneous dispersion of graphene flakes in water solution by means of the amphiphilic surfactant of sodium cholate having the hydrophobic head interacting with the hydrophobic graphene and the hydrophilic head associated to the aqueous environment [30]. The precipitation method for the synthesis of the metal oxides from their nitrate or acetate precursors requires the presence of a precipitation agent, like sodium hydroxide (NaOH) which is acting as a hydroxyl source for the conversion of the metal cations to metal hydroxides and finally to metal oxides, as it will be shown later. This work will show that the pH of the suspension will play also the role of nanostructure orientation for the Z-G hybrids, where nanoflower-like 3D architectures will be obtained for pH=14.

The synthesis of ZnO-1.4 wt% Graphene hybrid consisted in dissolving an amount of 0.894 grams of $Zn(NO_3)_2 \times 6\ H_2O$ in deionized (DI) water, which was then slowly added to 71.4 mL of aqueous solution of graphene, while the suspension was under stirring for about 15 minutes. Then, the NaOH which was initially dissolved in DI water was added droplet by droplet to the suspension until the pH reached the desired value. During entire sonochemical synthesis the volume of the suspension was kept constant to about 80 mL, which determined an intensity of acoustic radiation of about 2.5 W/mL of suspension. Thus, four suspensions were prepared having the pH value equal to 8.5, 10, 11.5 and 14.

Then, each suspension was exposed for about 1.5 hours to the sonochemical process of high acoustic irradiation density described above. In each case, the concentration of graphene in the matrix of ZnO-Graphene (Z-G) was about 1.4 wt%. A ZnO-Graphene precipitate was obtained for each of the four suspensions after washing and filtering in DI water a few times till the pH of the supernatant phase was equal to 7. The Z-G precipitate was dried at 150°C and calcinated in nitrogen for 1 h at 450°C. As such ZnO-Graphene nanocomposites could be used at higher temperatures in air, like in the case of sensing layers for chemiresistive gas sensor, a calcination at 450°C in air was also performed and evaluated. X-Ray-Diffraction (XRD) pattern of Z-G powders after drying and calcination has been obtained on a 9kW Rigaku SmartLab XRD System with rotating anode, while the Raman spectra on the same specimens have been acquired by Lab Ram HR 800 Raman spectrometer with a He-Ne laser excitation of wavelength equal to 633 nm. Scanning electron microscopy (SEM) has been used for surface morphology investigation and formation of nanostructured ZnO-Graphene as a function of the pH of the emulsion during sonochemical synthesis.

3 Results and Discussion

The experimental results of crystallization obtained from XRD analysis of the ZnO-1.4 wt% Graphene (Z-G) nanocomposites have been sensitive to the sonochemical processing conditions and composition of the hybrid, even if the hexagonal phase with wurtzite structure of zincite, specific to ZnO was found after drying at 150°C for all pH con-

ditions used during hybrid synthesis. Thus, in Figure 2, the XRD pattern of a ZnO-1.4 wt% Graphene powder prepared at pH=14, after drying at 150°C in air is shown. The angular positions of XRD peaks are 31.81, 34.49, 36.28, 38.64, 40.52, 47.63, 56.61, 62.85, 66.28, 67.97, 69.10, 72.5, 76.95 and 81.42° are in full agreement with the zinc oxide wurtzite structure [33], while the amount of graphene added for the Z-G synthesis is hardly influencing the XRD pattern of the Z-G hybrid.

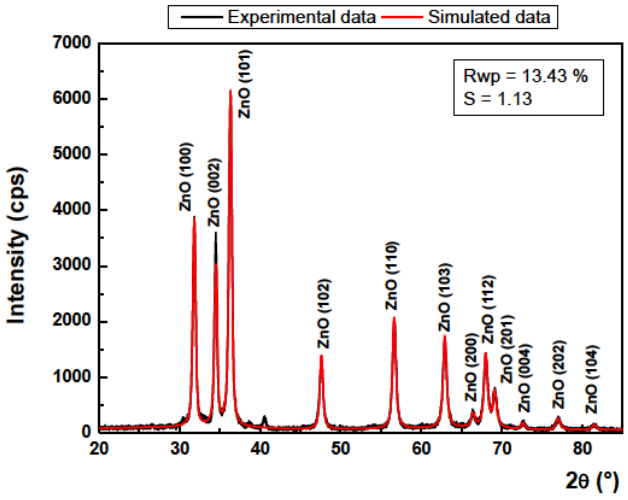

Figure 2: XRD pattern of ZnO-1.4wt% Graphene powder obtained at pH=14, after drying process at 150°C (black curve). Red curve stands for the simulated data using Rietveld analysis.

The crystallite size of 18 nm obtained from Debye-Scherrer equation on (101) atomic plane of this Z-G powder prepared at pH=14 was the highest value with respect to the Z-G hybrids prepared at lower pH values. The XRD patterns of the Z-G powders sonochemically prepared at pH values of 11.5, 10 and 8.5 have had a crystallite size in the range from 11 to 17 nm. In order to gain a deeper insight of the crystallite size, we considered all reflections using Rietveld refinement [34], which is based on a least squared method. The obtained results depend on the information held by each phase. The theoretical profile (red curve) was used to simulate the experimental data (black curve) with different fitting parameters using least squares fitting. The obtained values for R_{wp} and S, which are a measure of goodness of fit, are listed in the inset from figures for each sample.

Also, from Rietveld refinement it was obtained that the crystallite size increases with pH values as follows: 3.5 nm at pH = 8.5, 10.8 nm at pH = 10, 12.9 nm at pH = 11.5 up to 18.4 nm at pH = 14.

This systematic increase of Z-G crystallite size as a function of pH value of the suspension during sonochemical synthesis may be explained by the colloidal science in terms of electrical diffuse double layer (DDL) at the interface between each particle suspended in a liquid electrolyte, as follows [35]. Simply speaking the first "layer" of DDL consists of surface charge of the solid particle, while the second "layer" consists of counterions of that surface charge (including solvated counterions and solvent molecules) which are screening the surface charge. Some of the these counterions remain fixed to the surface charge while others are mobile due to combined effect of electrostatic forces and thermal motions. The electro-kinetic potential determined by the net charge included in the fix portion of the DDL is called zeta potential. It is this zeta potential which is determining the level of electrostatic repulsion between particles and finally the stability of the colloidal suspensions. Thus, if the zeta potential of a colloid is high, i.e. outside of the range of −40 mV; +40 mV, the electrostatic repulsion between particles in the suspension is high and therefore these particles will not aggregate each other. On the contrary, if the zeta potential is low, within the above voltage range, the particles will coagulate [36, 37].

Recently, it has been experimentally demonstrated that the particle size of the ZnO colloids has increased as a function of pH value of the suspension, while the zeta potential has decreased below +40mV with pH increase, entering the stability domain for pH >7. This result confirmed the general theory of zeta potential from above [38].

Therefore, our results showing the increase of the ZnO-Graphene nanoparticles size as a function of pH increase are in full agreement with the above colloidal theory and can be explained by means of the zeta potential evolution as a function of the pH of the suspension exposed to sonochemical process. We can thus deduce that the zeta potential of the sonochemically prepared ZnO-Graphene colloids has continuously decreased as a function of pH increase from 8.5 to 14, explaining the particle size increase with pH value.

On the other hand, it is known that during sonochemical synthesis performed in atmospheric ambient, the CO_2 from air is absorbed in the suspension and may react with hydroxyl anions and Zn^{2+} cations for creating zinc carbonate hydroxide (hydrozincite), $Zn_5(CO_3)_2(OH)_6$ [39]. It is also known that such a Zn compound will be decomposed to ZnO by thermal annealing at temperatures between 180 and 350°C [40]. It is interesting to note that the analysis of XRD pattern of Z-G powder prepared at pH=14, from Figure 2, showed that the amount of zinc carbonate hydroxide

was too small to be detected at the end of a drying process performed at 150°C, even if graphene was also there.

However, the analysis of XRD patterns at lower pH values has revealed not only the zincite phase, but also a weak "graphite" phase with a crystallite size increasing from 2.7 to 2.9 nm and to 9.1 nm, when the pH value was decreasing from pH=11.5, to pH=10 and pH=8.5, respectively. Such a "graphite" phase indicated by the XRD instrument may be a direct consequence of the presence of Zn carbonate hydroxide in the composition of the Z-G hybrid, in addition to graphene, immediately after drying process, at 150°C. In Figure 3, the XRD pattern of such a Z-G hybrid sonochemically prepared at a pH value equal to 8.5, containing weak carbon peaks at 26.42°, 40.58° and 54.21° is shown. The low intensity peaks of carbon compound, slightly above the noise background from Figure 3 demonstrate that a quite small amount of zinc carbonate hydroxide may be formed during the sonochemical process.

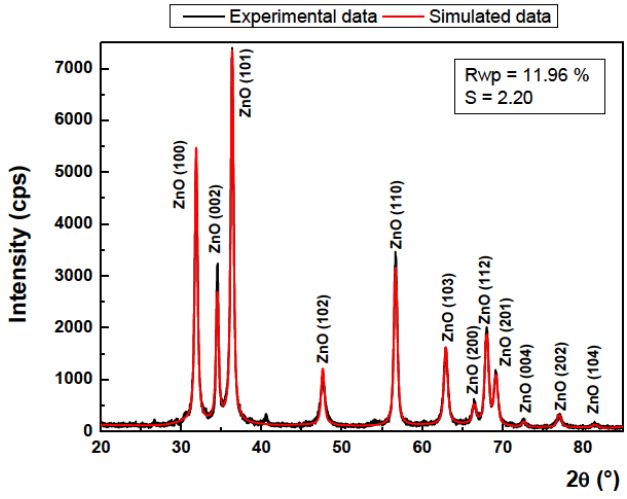

Figure 3: XRD pattern of ZnO-1.4wt% Graphene hybrid sonochemically prepared at pH= 8.5, after drying at 150°C. Red curve stands for the simulated data using Rietveld analysis.

The "graphite" phase, below the limit of detectability of XRD method for the composites prepared at pH=14 was the first indication of the important role played by the pH value in the composition and nanostructure formation for this hybrid. The thermal treatment of the Z-G hybrid in nitrogen at 450°C has converted most of the "graphite" phase into ZnO phase, and the XRD analysis proved that a very small amount of "graphite" was obtained for pH from 8.5 to 14 at the end of this annealing, even if the Raman spectra (to be shown later) have revealed the graphene with its specific vibration modes is still there. More convincing data on this aspect will be presented by energy dispersive X-ray spectroscopy (EDS), later. In the same time, the crystallite size of the Z-G hybrid thermally treated in N_2 at 450°C further increased, being in the range of 10-24 nm, with the highest value obtained, again, for the samples prepared at pH=14. A calcination process in air at 450°C performed on a sample sonochemically prepared at pH=10 has also provided the presence of zincite phase for Z-G hybrid, with a crystallite size equal to 10.8 nm. These XRD results, where the crystalline state was evinced before higher thermal treatments prove the important role of both sonochemical process, with its high local thermal and mechanical energies, and even the effect of the pH value on the nanostructure and crystallization of the ZnO-1.4 wt% Graphene.

Further, texture characterization was achieved using XRD and pole figures. Using all reflections from ZnO, the texture coefficient (TC) on (101) was derived using the following formula [41]:

$$TC_{(101)} = \frac{I_{101}/I^0_{101}}{\frac{1}{N}\sum I_{hkl}/I^0_{hkl}}, \quad (1)$$

where I_{hkl} are the observed peak relative intensities, I^0_{hkl} the relative intensities for the isotropic random oriented powder for reflection (hkl) and N is the number of considered Bragg reflections. In our case, we considered 12 reflections and we obtained values for TCs closely to unity at both pH of 8.5 and 14, which indicates that the investigated samples are poor-textured. The poor texture is also confirmed by pole figures (Figure 4), where the specific spots for hexagonal lattice of ZnO are absent. Although the atoms are almost randomly distributed, a flower-like shape in the pole figures can be remarked for both pH of 8.5 and 14.

The morphological investigations performed by SEM on Z-G hybrids sonochemically prepared at different pH values are presented in Figure 5 (a-d) after the drying at 150°C. These results have proved the preeminent role of the concentration of the hydroxyl anions in the crystal and nanostructure growth, in agreement with previous results on pure ZnO powders prepared by precipitation methods [42]. From Figure 5 (a), it is obvious that for sonochemical synthesis of Z-G nanocomposite at pH value equal to 14, well defined 3D architectures of nanoflowers-like are obtained in the absence of any chemical agent for nanostructure orientation. This nanoflower nanostructure can be explained by an anisotropy of ZnO-Graphene hybrid growth on certain directions perpendicular on a central seed, thus forming nanopetals with a certain length of 300-600 nm and width of 100-200 nm.

On the other hand, from Figures 5(c-d) one can note that when the pH of the suspension is decreasing, the ini-

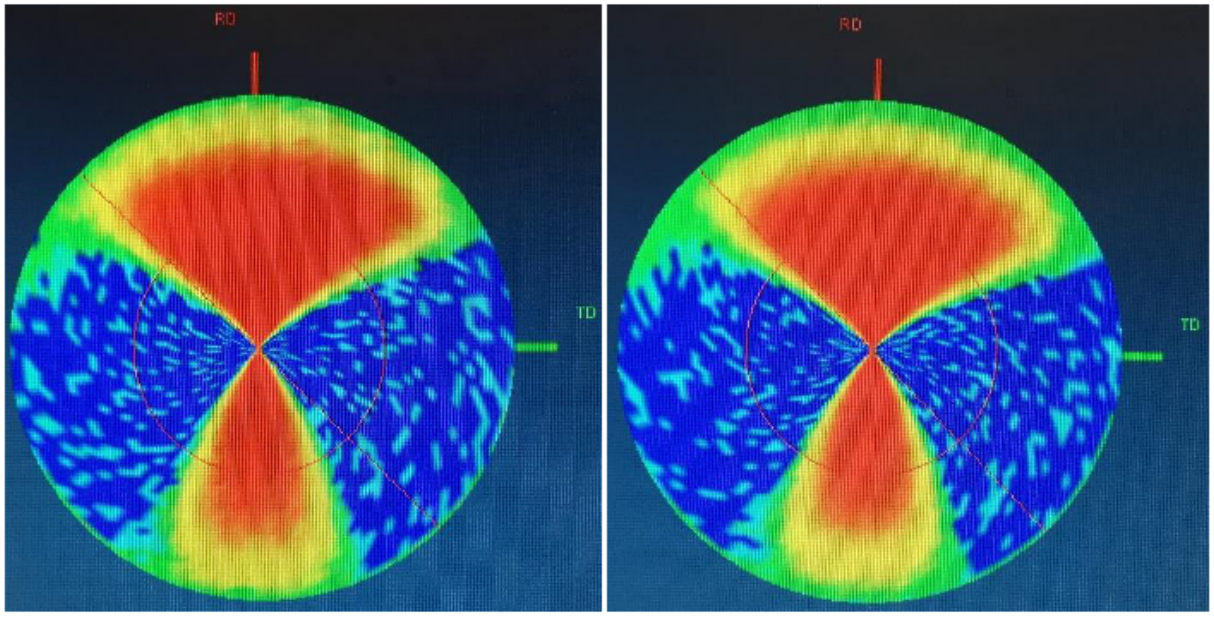

Figure 4: Pole figures recorded on (101) atomic plane. The schematic representation is made in 3D Explore software from Rigaku.

tial architecture is changed, as follows. The nanostructure of Z-G hybrid prepared at a pH value equal to 11.5 is still nanoflower-like preserving in a way a certain number of growth seeds, but in this case the anisotropy is not so high and the nanopetals are wider and touching one to the other. For a pH value equal to 10, the anisotropy of Z-G growth is almost vanished, and the nanostructure is a mixture of some remaining nanoflowers and nanopetals and many agglomerated particles with dimensions of 50-100 nm. Finally, for a pH value equal to 8.5, the entire nanostructure of Z-G hybrids consists mainly of nanopetals and nanoparticles with dimensions in the range of 50-500 nm.

A phenomenological model for the explanation of the above Z-G nanostructure formation should be mainly based on the evolution of the hydroxyl anions concentration [42] in the suspension during the sonochemical process, and the associated zeta potential of Z-G colloids. The graphene present in the suspension may act as a functionalization component of the ZnO crystal growth, further limiting the crystal growth, but not imposing the above nanostructure formation, which was directly correlated with the pH of the liquid phase.

The major chemical reactions leading to the above nanostructure evolution as a function of hydroxyl anions could be the following [39, 43]:

$$Zn(NO_3)_2(aq) \rightarrow Zn_{2+}(aq) + 2(NO_3)^-(aq) \quad (2)$$

$$NaOH \rightarrow Na^+ + OH^- \quad (3)$$

$$Zn^{2+} + 2OH^- \rightarrow Zn(OH)_2 \quad (4)$$

$$Zn(OH)_2 + 2OH^- \rightarrow Zn(OH)_4^{2-} \quad (5)$$

(if OH^- anions are in excess)

$$CO_2 + 2OH^- \rightarrow CO_3^{2-} + H_2O \quad (6)$$

$$5Zn^{2+}6OH^- + 2CO_3^{2-} \rightarrow Zn_5(CO_3)_2(OH)_6 \quad (7)$$

The experimental results from Figure 5 (a-d) suggest that the concentration of hydroxyl anions determines not only the zeta potential and particle flocculation, but also both the anisotropy of ZnO growth and the number of the active sites on a certain ZnO seed. Thus, an increased number of active sites on the same seed will explain the formation of an increased number of nanopetals, as shown schematically in Figure 6. Unlike the results described in work [44], where very many nanopetals are grown on the same seed, the presence of the graphene on such seed may limit the number nanopetals formed for the same nanoflower, as depicted in Figure 5 (a) for the sonochemical synthesis at pH value of 14. The energy dispersive X-ray spectroscopy (EDS) performed on the ZnO-1.4 wt% Graphene powders prepared at the pH values from 8.5 to 14 has revealed the elemental analysis of the Z-G hybrid confirming the major peaks of Zn and oxygen elements and also showing an interesting evolution of the carbon element, in agreement with the qualitative observations provided by XRD analysis. Thus, in Figure 7, the EDS spectra of Z-G hybrids prepared at different pH values are shown as a function of different thermal treatments. From this figure one can notice

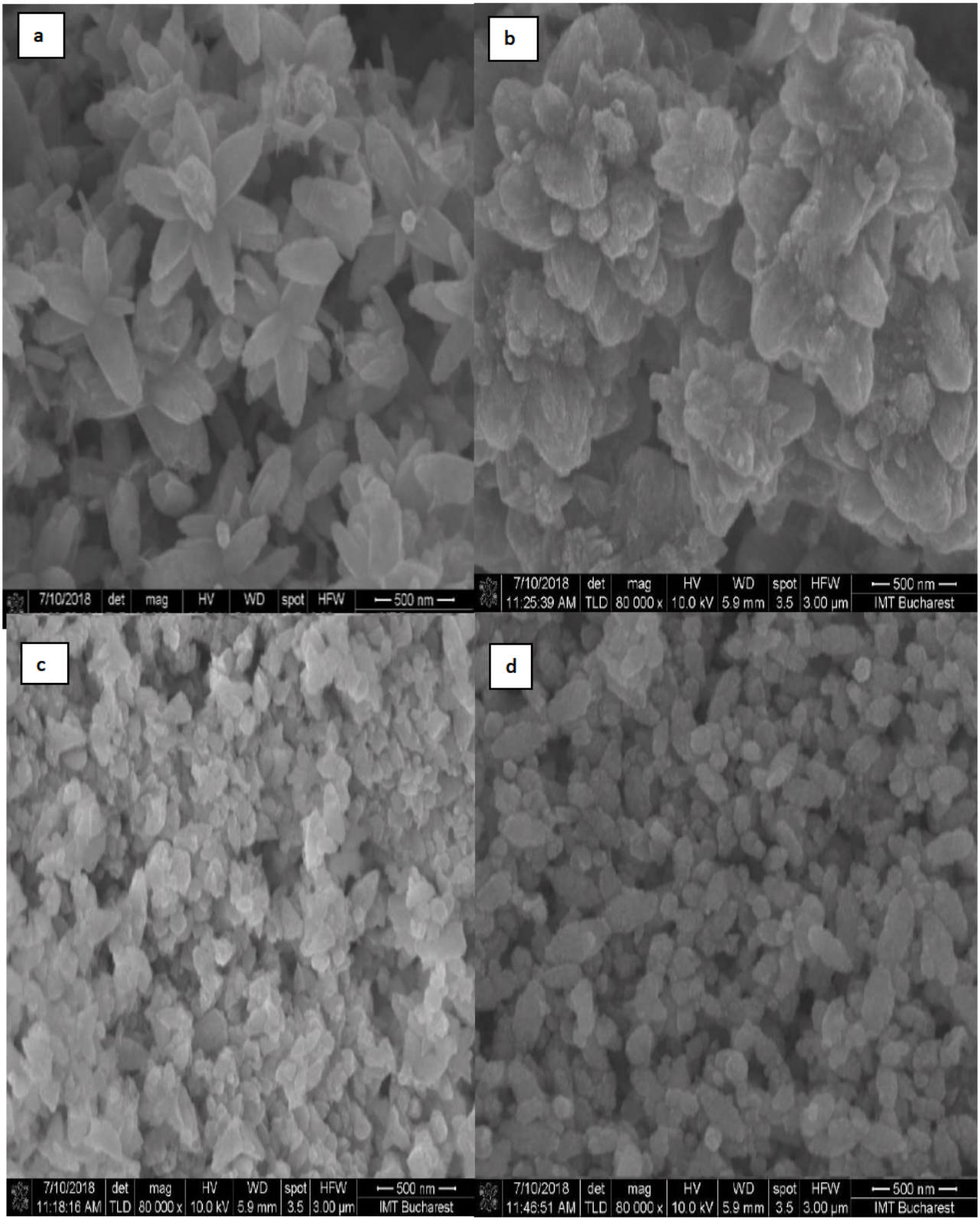

Figure 5: SEM images of the ZnO-1.4% Graphene nanocomposites sonochemically prepared at pH=14 (b) pH=11.5, (c) pH=10, (d) pH=8.5, after drying process at 150°C in air.

that after drying in air at 150°C, the Z-G hybrid obtained at pH=14 has the lowest peak of carbon which can be attributed to incorporated graphene, mainly, while its value is continuously increasing with the decrease in pH of suspension from 14 to 8.5 during sonochemical synthesis.

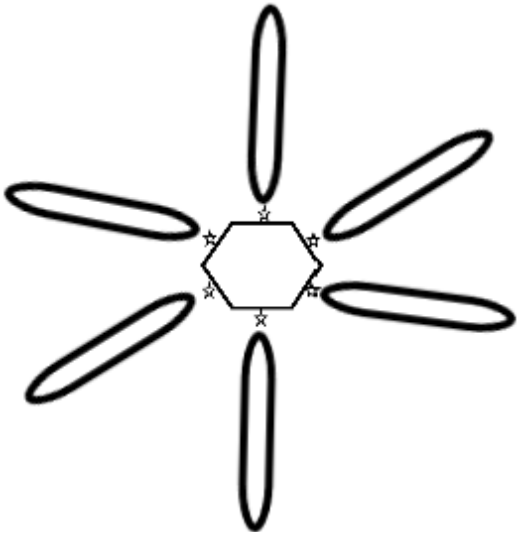

Figure 6: Schematic modelling of the nanoflower growth for high value of the pH of the suspension during sonochemical processing. The stars are the active sites and the hexagon is the ZnO nucleus.

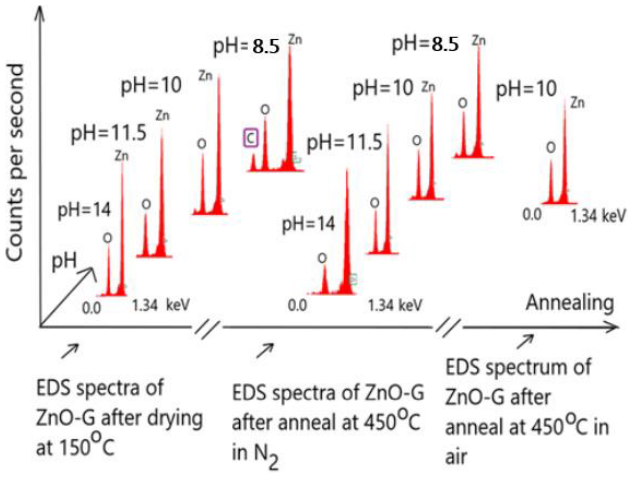

Figure 7: EDS spectra of ZnO-1.4wt% Graphene hybrids as a function of different thermal treatments in nitrogen or air.

Even if after 450°C annealing in N_2 of the Z-G hybrids the XRD results discussed above have hardy identified carbon above background noise, the EDS results from Figure 7 are still showing a residual amount of carbon which is very weakly increasing when the pH is decreasing from 14 to 8, and this may be due to annealing in nitrogen of Z-G hybrid, and not in air. However, after calcination in air at 450°C, the EDS spectra of Z-G hybrid from Figure 7 did not indicate any peak of carbon, due to conversion of zinc carbonate hydroxide (hydrozincite) to ZnO, in agreement with the work [40]. For better understanding the formation of the ZnO-Graphene nanocomposite, Raman spectroscopy was performed on ZnO-1.4 wt% Graphene hybrids prepared by sonochemical synthesis as a function of pH of the suspension, after drying in air at 150°C and after thermal annealing at 450°C in either nitrogen or air ambient.

Thus, in Figure 8, the Raman spectra of the ZnO-1.4% Graphene hybrids prepared at different pH values from 8.5 to 14 and dried at 150°C in air are shown. These results indicate that in the case of ZnO-Graphene hybrids, prepared at pH values from 8.5 to 11.5 only the Raman bands of graphene are evidenced as follows : D (1325-1329) cm^{-1}, G (1571-1681) cm^{-1}, G^+ (1602-1617) cm^{-1}, 2D (2638-2651) cm^{-1} , D+G (2905-2913) cm^{-1}. The split of the G band into two bands G and G^+ as well as the greater height of the D defect peak with respect to G peak can be associated to the high number of defects introduced by the sonochemical process on the atomic arrangement of graphene flakes. Such a split of the G band was also found in the Raman spectra of the commercial graphene consisting of 1-4 layers graphene flakes in aqueous solution [30], and this could be also associated with the fabrication method of the graphene flakes from graphite, where horn sonication of graphite was used. The rather similar height of 2D Raman peak from Figure 8 obtained at different pH values indicate that the thickness of the graphene flake is not changes during ZnO-graphene hybrid formation by sonochemical method. The absence of the ZnO Raman bands for the Z-G hybrid for the pH values from 8.5 up to 11, after the drying process at 150°C was rather unexpected considering the XRD findings, where diffraction peaks of the ZnO were identified, as shown in Figure 3 from above. This result may be explained by the defect structure of the hybrid and maybe by the decreased or even lack of nanostructure formation for such low pH values, as revealed by the SEM images from Figure 5 (b-d). As shown in Figure 8, the Raman band of ZnO from 314.9 cm^{-1} with a broad peak associated to multiphonon process [45] and the 428.2 cm^{-1} band associated to optic vibration modes (E2 high mode [46] are revealed for the Z-G hybrids prepared at pH value equal to 14, where nanoflower 3D architectures are also obtained. This E2 high mode with a broad peak may indicate that the ZnO atomic ordering process is still in the early stage after drying process, even if a nanoflower formation has been obtained.

The Raman spectra of the ZnO-Graphene powders after temperature treatment at 450°C in nitrogen are shown

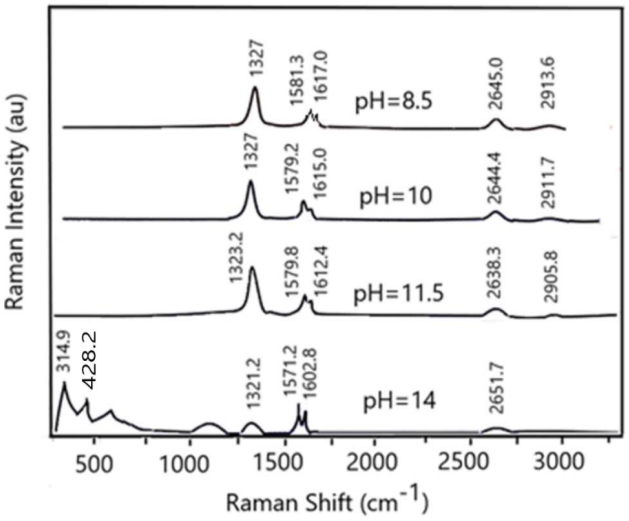

Figure 8: Raman spectra of ZnO-1.4wt% Graphene hybrids after drying process in air at 150°C, for different pH values during synthesis.

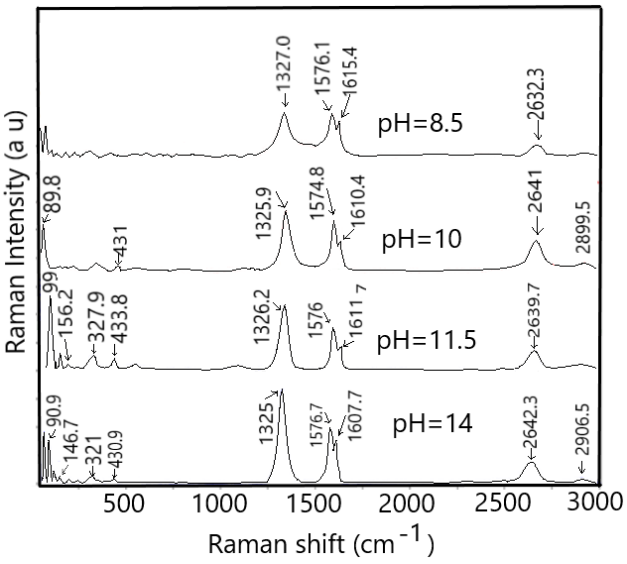

Figure 9: Raman spectra of ZnO-1.4 wt% Graphene hybrids after thermal treatment in nitrogen at 450°C, for different pH values of the suspension during sonochemical synthesis.

in Figure 9 for different values of the pH value during sonochemical synthesis of the Z-G hybrid. From this figure it is noticed that at a pH value equal to 8.5 the Raman spectra of ZnO are still silent, even if there is a weak tendency that the peak associated to low mode of heavy Zn sublattice to exist [42]. With the increase of the pH value of the suspension from 8.5 to 14 during the sonochemical synthesis of ZnO-Graphene composite, the number of Raman active bands of ZnO is increasing, being similar for pH values equal to 11.5 and 14. The optical modes from 90-99 cm^{-1} and 430-434 cm^{-1} found in these spectra are associated to E2 (low) mode and E2 (high) modes of the zinc sublattice and oxygen sublattice, respectively, and their presence is an indication of the development of the crystallization process. The Raman band from 321-327 cm^{-1} associated to multiphonons process [45] which was found in samples from pH=11.5 and 14 (Figure 9) was much sharper after the 450°C annealing in nitrogen process with respect to the same band found in Z-G hybrid from pH equal to 14 an after drying process, and this change in the shape of the band is associated to the crystallization process.

The very weak Raman band from 145-156 cm^{-1} from Figure 9, for the 450°C-N_2 annealed Z-G hybrid prepared at pH values of 11.5 and 14, not previously described in the literature, might be correlated with the ZnO wurtzite crystallization process in the presence of the graphene.

One of the key issues in the use of ZnO-Graphene nanocomposites for different gas sensing applications is the chemical stability of the hybrid used as sensing layer, when this is exposed to higher temperatures in air, as it is the case of chemiresistive sensors [47]. For this reason, in Figure 10, the Raman spectra of the ZnO-Graphene nanocomposite treated at 450°C in air for a pH value equal to 10 and is shown. The Raman spectra for the Z-G hybrid after this high temperature treatment in air prove that the graphene fingerprint has decreased, with a relatively weak G band surviving at 1575.1 cm^{-1}. After calcination in air, the Raman band from 91 cm^{-1} was very narrow and its intensity was very high suggesting the highest stoichiometry of the ZnO matrix, due to further oxygen atoms coming from the air and filling the lattice vacancies. Thus, the higher order and symmetry in the atomic arrangement of the ZnO network may explain the high value of the band from 99 cm^{-1}. The major changes in the Raman bands of graphene are explained by the fact that the onset of graphene oxidation in air starts at about 250°C [48], and this oxidation process is revealed in Figure 10 by almost disappearance of specific Raman bands of graphene. In addition, the possible zinc hydrozincite formed during sonochemical process was decomposed during the thermal treatment in air at 450°C according to the reaction from below and thus being converted into ZnO [49]:

$$Zn_5(CO_3)_2(OH)_6 \rightarrow 5ZnO + 2CO_2 + 3H_2O \qquad (8)$$

From Figure 10 one can also notice the presence of a new Raman band at 1078.4 cm^{-1}, which was assigned in the literature to the acoustic combination of the A1 mode, as a polar transversal optic mode and E2 optic mode associated to the vibrations of ZnO lattice [46]. Such a Raman active band from 1078 cm^{-1} which was not seen before this thermal annealing in air at 450°C may suggest the relative conversion of the ZnO-Graphene composite into more stoichio-

metric ZnO crystal, after the partial oxidation of graphene and conversion of the hydrozincite into ZnO as described in the equation (8) from above.

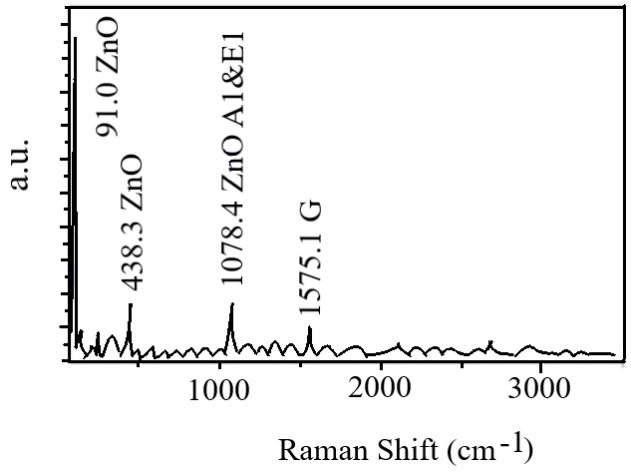

Figure 10: Raman spectra of the ZnO-1.4 wt% hybrid after thermal treatment in air at 450°C.

In agreement with previous fundamental studies, the above Raman spectra of the ZnO-Graphene hybrid prove the chemical instability of the Z-G material when treated at 450°C in air. As a practical conclusion, the ZnO-Graphene hybrid used as a sensing layer in chemiresistive sensors should not be heated above the onset temperature of the graphene reaction with oxygen of about 250°C.

4 Conclusions

The present paper has presented the morphological, structural and compositional properties of the ZnO-1.4wt% Graphene nanocomposites prepared by sonochemical method from aqueous solutions of zinc nitrate and commercial graphene with 1-4 layers as a function of pH value of the suspension during synthesis, from 8.5 up to 14, and different thermal annealing in nitrogen and air up to 450°C.

By interpretation of the experimental results of XRD, EDS, SEM and Raman spectroscopy, the following findings could be mentioned here as follows.

The sonochemical synthesis of the Z-G hybrid at high density of acoustic radiation has determined a crystallization process of the as-prepared nanocomposite, with particle size increasing from 3.5 nm to 18 nm, when pH increased from 8.5 to 14. The result was explained in terms of zeta potential decrease as a function of pH increase. During synthesis, the CO_2 from the air was absorbed in the liquid phase and determined the increased carbon concentration in the Z-G powder, beyond contribution of graphene itself. A possible hydrozincite phase was proposed to be formed by this process. The XRD and EDS analyses of the Z-G nanocomposite after the drying at 150°C in air have indicated the presence of this total carbon in the composition, and its amount has increased with the pH decrease from 14 to 8.5. The amount of total carbon in the Z-G hybrid has decreased after N_2 treatment at 450°C in N_2, but the same trend of increased amount for pH value decreasing from 14 to 8.5 was kept, as revealed by EDS spectra, while the graphene composition, as revealed by Raman spectra, was not affected. The thermal annealing of the Z-G hybrid in air at 450°C has burned most of the carbon from the composition, including most of the graphene content.

The SEM analysis of the Z-G hybrids has shown the strong role of the pH value of the suspension in the development of nanostructures, where nano-flower like 3D architectures were obtained at pH equal to 14, without addition of any orientation agents. With the decrease of pH value, the nanoflowers with high particle growth anisotropy degenerated into nanoflowers with wide petals at pH equal to 11.5 and then to dispersed nanopetals at pH equal to 10 and finally to agglomerated nanoparticles at pH equal to 8.5. An intuitive model for the nanoflower growth was proposed, where the number of active sites on a ZnO seed increased with the increase of hydroxyl anions concentration in the suspension, which also determined the decrease of zeta potential and associated flocculation process.

The Raman spectroscopy has clearly demonstrated the formation of the Z-G nanocomposite, indicating also the important role of pH value in the nanostructure formation. Thus, at lower values of pH, from 8.5 up to 11, the ZnO-specific Raman active bands were not evinced for the Z-G hybrids dried at 150°C. Some of the important Raman bands for ZnO started to be seen only for the dried powder prepared at pH equal to 14, proving thus the role of atomic arrangement and symmetry given by nanoflower-like nanostructure. Moreover, even after the thermal annealing at 450°C in N_2, the role of pH was still evident, as the number of ZnO Raman active bands has increased as a function of pH value increase.

The experimental study has shown that for practical applications of the ZnO-Graphene nanocomposites, like chemiresistive gas sensing, it is essential to limit the exposure of the material much below 450°C in air, in order to prevent the oxidation of graphene and thus preserve the chemical composition of the Z-G hybrid.

Acknowledgement: The authors would like to thank to the Romanian Ministry of Education and Research for the financial support of the "NUCLEU" research program "MICRO-NANO-SIS PLUS", Cod PN 19 16, to which the present research is assigned.

References

[1] Seiyama, T., A. Kato, K. Fujiishi, and M. Nagatani. A New Detector for Gaseous Components Using Semiconductive Thin Films. *Analytical Chemistry*, Vol. 34, No. 11, 1962, pp. 1502–1503.

[2] Wan, Q., Q. H. Li. Y. J. Chen, T. H. Wang, X. L. He, J. P. Li, et al. Fabrication and ethanol sensing characteristics of ZnO nanowire gas sensors. *Applied Physics Letters*, Vol. 84, 2004, pp. 3654–3656.

[3] Wang, Z. L., and J. Song. Piezoelectric nanogenerators based on zinc oxide nanowire arrays. *Science*, Vol. 312, No. 5771, 2006, pp. 242–246.

[4] Özgür, Ü., Y. I. Alivov, C. Liu, A. Teke, M. A. Reshchikov, S. Doğan, et al. A comprehensive review of ZnO materials and devices. *Journal of Applied Physics*, Vol. 98, No. 4, 2005, 041301.

[5] Liu, C., A. Zapien, Y. Yao, X. Menq, C. S. Lee, S. Fan, Y. Lifshitz, and S. T. Lee. High-Density, Ordered Ultraviolet Light-Emitting ZnO Nanowire Arrays. *Advanced Materials*, Vol. 15, No. 10, 2003, pp. 838–841.

[6] Liang, H. K., S. F. Yu, and H. Y. Yang. Directional and controllable edge-emitting ZnO ultraviolet random laser diodes. *Applied Physics Letters*, Vol. 96, No. 10, 2010, 101116–101118.

[7] Chu, D., Y. Masuda, T. Ohji, and K. Kato. Formation and Photocatalytic Application of ZnO Nanotubes Using Aqueous Solution. *Langmuir*. Vol. 26, No. 4, 2010, pp. 2811-2815.

[8] Abbasi, S., M.-S. Ekrami-Kakhki, and M. Tahari. Modeling and predicting the photodecomposition of methylene blue via ZnO–SnO_2 hybrids using design of experiments (DOE). *Journal of Materials Science Materials in Electronics*, Vol. 28, No. 3, 2017, pp. 15306–15312.

[9] Fakhrzad, M., A. H. Navidpour, M. Tahari, and S. Abbasir. Synthesis of Zn_2SnO_4 nanoparticles used for photocatalytic purposes. *Materials Research Express*, Vol. 6, No. 9, 2019, p. 095037.

[10] Abbasi S. Photocatalytic removal of methyl orange in suspension containing ZnO and SnO_2 nanoparticles and investigation the influence of effective variables on the process. *Iranian Journal of Health and Environment*, Vol. 9, Issue 3, 2016, pp. 433–442.

[11] Ghaderi, A., S. Abbasi, and F. Farahbod. Synthesis of SnO_2 and ZnO Nanoparticles and SnO_2-ZnO Hybrid for the Photocatalytic Oxidation of Methyl Orange. *Iranian Journal of Chemical Engineering*, Vol. 12, 2015, pp. 96–105.

[12] Ghaderi, A., S. Abbasi, and F. Farahbod. Synthesis, characterization and photocatalytic performance of modified ZnO nanoparticles with SnO 2 nanoparticles. *Materials Research Express*, Vol. 5, No. 6, 2018, p. 065908.

[13] Abbasi, S., and M. Hasanpour. The effect of pH on the photocatalytic degradation of methyl orange using decorated ZnO nanoparticles with SnO_2 nanoparticles. *Journal of Materials Science Materials in Electronics*, Vol. 28, No. 2, 2017, pp. 1307–1314.

[14] Manjon, F. J., B. Mari, J. Serrano, and A. H. Romero. Silent Raman modes in zinc oxide and related nitrides. *Journal of Applied Physics*, Vol. 97, No. 5, 2005, 053516–4.

[15] Gayathri, S., P. Jayabal, M. Kottaysami, and V. Ramaakrishnan. Synthesis of ZnO decorated graphene nanocomposite for enhanced photocatalytic properties. *Journal of Applied Physics*, Vol. 115, No. 17, 2014, 173504–173509.

[16] Huang, J., T. Yang, Y. Kang, Y. Wang, and S. Wang. Gas sensing performance of polyaniline/ZnO organic-inorganic hybrids for detecting VOCs at low temperature. *Journal of Natural Gas Chemistry*, Vol. 20, No. 5, 2011, pp. 515–519.

[17] Li, Q., Y. Li, and M. Yang. Tin oxide/graphene composite fabricated via a hydrothermal method for gas sensors working at room temperaturę. *Sensors and Actuators. B, Chemical*, Vol. 173, 2012, pp. 139–147.

[18] Dutta, M., S. Sarkar, T. Ghosh, and D. Basak. ZnO/Graphene Quantum Dot Solid-State Solar Cell. *Journal of Physical Chemistry C*, Vol. 116, No. 38, 2012, pp. 20127–20131.

[19] Neri, G. First Fifty Years of Chemoresistive Gas Sensors. *Chemosensors (Basel, Switzerland)*, Vol. 3, No. 1, 2015, pp. 1–20.

[20] Hieu, N. V., L. T. B. Thuy, and N. D. Chien. Highly sensitive thin film NH_3 gas sensor operating at room temperature based on SnO_2/MWCNTs composite. *Sensors and Actuators. B, Chemical*, Vol. 129, 2008, pp. 888–895.

[21] Guo, J., Y. Li, S. Zhu. Z. Chen, Q. Liu, D. Zhang, et al. Synthesis of WO_3@Graphene composite for enhanced photocatalytic oxygen evolution from water. *RSC Advances*, Vol. 2, 2012, pp. 1356–1363.

[22] Abbasi, S., M. Hasanpour, and M.-S. Ekrami-Kakhki. Removal efficiency optimization of organic pollutant (methylene blue) with modified multi-walled carbon nanotubes using design of experiments (DOE). *Journal of Materials Science Materials in Electronics*, Vol. 28, No. 13, 2017, pp. 9900–9910.

[23] Abbasi, S. Adsorption of dye organic pollutant using magnetic ZnO embedded on surface of graphene oxide. Journal of Inorganic and organometallic. *Polymers*, 2019, https://doi.org/10007/S10904-019-01336-4.

[24] Abbasi, S., and M. Hasanpour. Variation of the photocatalytic performance of decorated MWCNTs (MWCNTs-ZnO) with pH for photo degradation of methyl orange. *Journal of Materials Science: Materials in Electronics*, Vol. 28, 2017, 11846–11855.

[25] Roozban, N., S. Abbasi, and M. Ghazizadeh. The experimental and statistical investigation of the photo degradation of methyl orange using modified MWCNTs with different amount of ZnO nanoparticles. *Journal of Materials Science Materials in Electronics*, Vol. 28, 2017, pp. 7343–7352.

[26] Roozban, N., S. Abbasi, and M. Ghazizadeh. Statistical analysis of the photocatalytic activity of decorated multi-walled carbon nanotubes with ZnO nanoparticles. *Journal of Materials Science Materials in Electronics*, Vol. 28, 2017, pp. 6047–6055.

[27] Abbasi, S. Investigation the Kinetic Reaction Variation of the Methyl Orange Decomposition Using Decorated Multi-Walled Carbon Nanotubes with ZnO Nanoparticles, Influence of Nanoparticle. *Journal of Environmental Health Engineering*, Vol. 5, No. 2, 2018, pp. 113–122.

[28] Abbasi, S., and F. Ahmadpoor. M. Imani and & M.S. Ekrami-Kakhki. *International Journal of Environmental Analytical Chemistry*, Vol. 100, 2020, pp. 225–240.

[29] Bang, J. H., and K. S. Suslick. Applications of ultrasound to the synthesis of nanostructured materials. *Advanced Materials*, Vol. 22, No. 10, Mar. 12, 2010, pp. 1039–1059.

[30] Green, A. A., and M. C. Hersam. Solution phase production of graphene with controlled thickness via density differentiation.

Nano Letters, Vol. 9, No. 12, 2009, pp. 4031–4036.
[31] Cobianu, C., B-C Serban, A. Stratulat, V-G Dumitru, M. Brezeanu, and O. Buiu, US Patent 9,604191 B2, granted on 28 March 2017.
[32] Cobianu, C., B-C Serban et al, Romanian patent pending, 2018.
[33] Guo, L., Y. L. Ji, H. Xu, P. Simon, and Z. Wu. Regularly shaped, single-crystalline ZnO nanorods with Wurtzite structure. *Journal of the American Chemical Society*, Vol. 124, No. 50, 2002, pp. 14864–14865.
[34] Rietveld, H. M. A profile refinement method for nuclear and magnetic structures. *Journal of Applied Crystallography*, Vol. 2, No. 2, 1969, pp. 65–71.
[35] Lyklema, J. Fundamentals of Interface and Colloid Science: Solid-Liquid Interfaces: Vol 2 (Fundamentals of Interface & Colloid Science). Academic Press, 1995.
[36] Kumar, A., and C. K. Dixit. Methods for characterization of nanoparticles. Advances in Nanomedicine for the Delivery of Therapeutic Nucleic Acid, 2017, pp. 43–58.
[37] Greenwood, R., and K. Kendall. Selection of Suitable Dispersants for Aqueous Suspensions of Zirconia and Titania Powders using Acoustophoresis. *Journal of the European Ceramic Society*, Vol. 19, No. 4, 1999, pp. 479–488.
[38] Masalek, R. Particle Size and Zeta Potential of ZnO. *APCBEE Procedia*, Vol. 9, 2014, pp. 13–17.
[39] Pholnaka, C. C. Sirisathitkula, S. Suwanboonb, and D. J. Hardinga. Effects of precursor concentration and reaction time on sonochemically synthesized ZnO nanoparticles. *Materials Research*, Vol. 17, No. 2, 2014, pp. 405–411.
[40] Alhawia, T., M. Rehana, D. Yorka, and X. Laia. Hydrothermal Synthesis of Zinc Carbonate Hydroxide Nanoparticles. *Procedia Engineering*, Vol. 102, 2015, pp. 356–361.
[41] Hong, J.-I., J. Bae, Z. L. Wang, and R. Snyder. Room-temperature, texture-controlled growth of ZnO thin films and their application for growing aligned ZnO nanowire arrays. *Nanotehnology*, Vol. 20, No. 8, 2009, p. 085609.
[42] Liu, J., X. Huang, Y. Li, J. Duan, and H. Ai. Large-scale synthesis of flower-like ZnO structures by a surfactant-free and low-temperature process. *Materials Chemistry and Physics*, Vol. 98, No. 2-3, 2006, pp. 523–527.
[43] Zhang, H., D. Yang, X. Ma, Y. Ji, J. Xu, and D. Que. Synthesis of flower-like ZnO nanostructures by an organic-free hydrothermal process. *Nanotechnology*, Vol. 15, No. 5, 2004, pp. 622–626.
[44] Wu, W.-Y., W.-Y. Kung, and J.-M. Ting. Effect of pH Values on the Morphology of Zinc Oxide Nanostructures and their Photoluminescence Spectra. *Journal of the American Ceramic Society*, Vol. 94, No. 3, 2011, pp. 699–703.
[45] Calleja, J. M., and M. Cardona. Resonant Raman scattering in ZnO. *Phys. Rev. B*, Vol. 16, No. 8, 1977, pp. 3753–3761.
[46] Zhang, R., P.-G. Yin, N. Wang, and L. Guo. Photoluminescence and Raman scattering of ZnO nanorods. *Solid State Sciences*, Vol. 11, No. 4, 2009, pp. 865–869.
[47] Anand, K., O. Singh, M. P. Singh, J. Kaur, and R. C. Singh. Hydrogen sensor based on graphene/ZnO nanocomposite. *Sensors and Actuators. B, Chemical*, Vol. 195, 2014, pp. 409–515.
[48] Yamada, Y., K. Murota, R. Fujita, J. Kim, A. Watanabe, M. Nakamura, et al. Subnanometer vacancy defects introduced on graphene by oxygen gas. *Journal of the American Society*, Vol. 136, 2014, pp. 2232–2235.
[49] Hales, M. C., and R. L. Frost. Thermal analysis of smithsonite and hydrozincite. *Journal of Thermal Analysis and Calorimetry*, Vol. 91, No. 3, 2008, pp. 855–860.